Design and Analysis of a 100kW Rotary Transformer for XROTOR Wind Generators

Yang Teng
Electronic and Electrical Engineering
University of Strathclyde, Glasgow, UK
yang.teng@strath.ac.uk

Reza Yazdanpanah
Electronic and Electrical Engineering
University of Strathclyde, Glasgow, UK
reza.yazdanpanah@strath.ac.uk

Seyed Abolfazl Mortazavizadeh
Electronic and Electrical Engineering
University of Strathclyde. Glasgow, UK
seyed.mortazavizadeh@strath.ac.uk

Olimpo Anaya-Lara
Electronic and Electrical Engineering
University of Strathclyde
Glasgow, UK
olimpo.anaya-lara@strath.ac.uk

David Campos-Gaona
Electronic and Electrical Engineering
University of Strathclyde
Glasgow, UK
d.campos-gaona@strath.ac.uk

***Abstract*—This paper presents a design methodology for a high power rotary transformer solution for novel offshore X-rotor wind turbine. The design methodology is studied for both in 2D and 3D finite element method for a 100KW system. The results of current, voltage, output power and magnetic field in 2D model is the same as 3D model. The results verify the design methodology, and that efficiency is high enough to present the rotary transformer solution as an alternative for slip rings in the novel X-rotor wind turbine design. Also, the sensitivity analysis has been performed to show the effect of some important parameters.**

Keywords—high power, high efficiency, rotary transformer, sensitivity analysis, X-rotor.

I. INTRODUCTION

The X-rotor is a novel hybrid wind turbine concept that retains some of the advantages of a VAWT[1][2]. As depicted in Fig 1 the X-rotor concept has a primary vertical axis rotor consisting of an upper and lower part with relatively conventional blades that are angled both upwards and downwards from the ends of a relatively short, stiff cross-arm. The role of the upper part is to provide the major contribution to mechanical power extraction from the wind. Secondary horizontal axis rotors are attached to the lower blades of the primary rotor, which extract wind energy[3]. This design reduces the overturning moment on the main bearing and reduces the size and weight of the rotor, thus saves the cost of maintenance and installation. Furthermore, it can capture more energy from the wind, which greatly improves the efficiency of the machine.

One requirement in the X-rotor operation is the capacity to transfer the power generated by the secondary rotors from a rotating structure (the primary rotor) to the turbine tower. This can be done using a brush slip ring arrangement, however, there are many drawbacks of using slip rings in an offshore environment, where operation and maintenance costs are known to be much higher than in onshore systems. The drawbacks include sensibility to non-conductive oxide and friction, risk of short circuits, including spark discharge, local overheating and uneven wear.

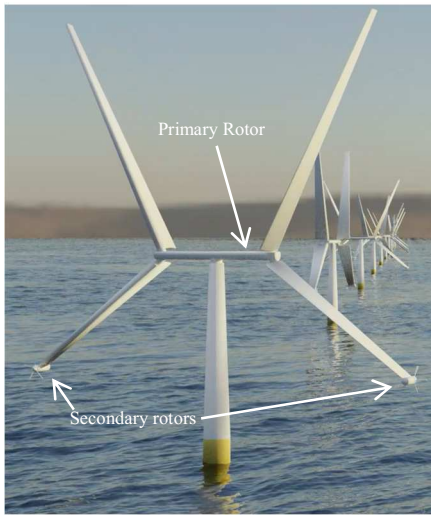

Fig 1. The X-rotor Offshore wind turbine

In order to solve the shortcomings of brush slip ring, a variety of non-contact methods have been proposed in the literature [1] - [7]. Such solutions rely on wireless power transmission technology using either capacitive or inductive principles. For near-field Wireless Power Transfer (WPT) the magnetic field coupling between the two coils can achieve energy transmission at high efficiency. This solution has been presented as a suitable replacement for slip rings and reduction of maintenance costs [6].

The objective of this paper to develop a rotary transformer design methodology capable of handling the power transfer requirements of X-rotor wind turbines at high efficiency levels (i.e. larger than 95%) over their operating range. To test the design methodology, a 600V/100kW rotary transformer is be designed and its performance is tested in 2D model and 3D models using Ansys Maxwell.

The structure of this paper is as follows: section II presents the analytical design procedure of single-phase high-power rotary transformer developed in this research. Also, some discussion on 2D model and 3D model and results are presented. Furthermore, to better appreciate the strengths and weaknesses of the design methodology, a sensitivity analysis of the results is

carried out in section III. Finally, the conclusions of this research are presented in section IV.

II. METHODOLOGY

A. Design procedure

For sinusoidal waveforms of current and voltage, the voltage V_{rms} of a N turns winding rotary transformer can be defined based on Faraday's Law as:

$$V_{rms} = \sqrt{2}\pi f N B_{max} A_C \ (V) \tag{1}$$

Where f is the supply frequency in Hz, A_C is the minimum core cross section area of the rotary transformer in mm^2 and B_{max} is the amplitude of operating magnetic flux density in the transformer core in Tesla.

The current density J of a conductor is calculated as:

$$J = \frac{I_m}{S_w} \ (A/mm^2) \tag{2}$$

Where I_m is the maximum current flow through the conductor in amperes, in turn, S_w is the conductor cross section area in mm^2.

For a one-phase transformer, the maximum current flow through the conductor is:

$$I_m = \frac{P_{trans}}{V_{rms}} \ (A) \tag{3}$$

Where P_{trans} is the transferred output power of the rotary transformer in Watts.

The window area of the primary core (Fig. 2) can be calculated based on the following equation:

$$A_w = \frac{N I_m}{k_f J} \ (mm^2) \tag{4}$$

Where k_f is the winding fill factor, usually 0 to 1.

The window area needed for the windings is calculated based on the calculated number of turns, the current density, and fill factor. The fill factor influences considerably the length of the window, a suitable fill factor makes a sufficient length of the window area that allows fitting all the copper inside the core area.

To define a sufficient window area, the first step is to set the value of width of the window area, that is:

$$b = n l_c + 3 (n = 2,4,6,8 \dots) \tag{5}$$

Where n considers multiple layers, n is equal to 2 in this case. As seen in Fig. 2, the cross-section area of the windings is a square area, thus the length of the conductor is calculated as:

$$l_c = \sqrt{S_w} \tag{6}$$

Based on (4) and (6), the length of the window area is

$$l_N = \frac{A_w}{b} \tag{7}$$

Assuming that all the turns are close to each other, the length of the winding is defined as:

$$l_{winding} = \frac{N l_c}{n_{layer}} \left(n_{layer} = 1,2,3,4 \dots\right) \tag{8}$$

n_{layer} is the number of layers for each winding. Comparing the results of (8) and (9), if l_N is larger than $l_{winding}$, then the window area is sufficient for the windings, otherwise we need to reduce the core cross section area A_C in order to increase the window area. In this regard [8] presents further information on the geometry and magnetic circuit representation of radial core type of the rotary transformer.

As seen in Fig. 2, the primary side of the cross-section area, A_{C1}, depends on the radius of the rotary transformer shaft R_{sh} and the outer radius of the primary side core R_1.

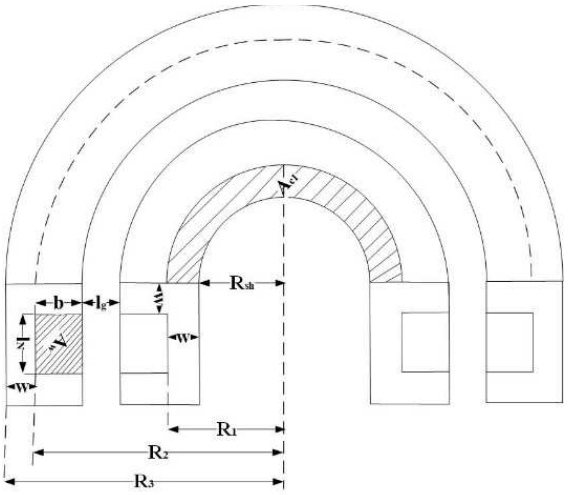

Fig. 2. Radial type single-phase rotary transformer

Finally, the copper loss of rotary transformer can be calculated as[9]:

$$copper_{loss} = \frac{\rho_c N MLT (J S_w)^2}{S_w} \tag{9}$$

where ρ_c is the resistivity of the conductor and MLT is the mean length of turn in one winding. MLT is calculated as:

$$MLT = 2\pi(R_1 + \frac{b}{4}) \tag{11}$$

Litz wire contains hundreds to thousands of individual strands of copper wire. Normally Litz wire could be used in higher frequency windings up to 1 MHz, to reduce AC losses as operating frequencies increase. They could also reduce the eddy current losses caused by skin effect and lower the operating temperature.

Proper model meshing and time step selection will eliminate the additional harmonics in the voltage and current waveforms and deploy faster simulations and results. This includes currents, voltages, losses and magnetic field intensity at different time intervals.

B. Design results

A single-phase high-power rotary transformer of 600V/100 kW is designed analytically and simulated in Ansys Maxwell using the methodology presented in section II. A. The design parameters are given in Table I, the Steel Alloy M250-35A was selected for the core and copper conductors was selected for the winding. An initial operating flux density of 0.7 T as was selected as adequate for the core material. However this value could be increased to produce small transformer.

The results of the dimension calculation are given in Table I. The designed considered an airgap at mm level to reduce the effects on leakage inductances and extra losses.

TABLE I. PARAMETERS OF 100 KW ROTARY TRANSFORMER

Symbol	Definition	Value
	input parameters	
V_{rms}	RMS voltage	600 V
P_{trans}	desired transferred power	100 kW
B_{max}	operating flux density	0.7 T
f	frequency	2000 Hz
k_f	winding fill factor	0.28
J	current density	4 A/mm^2
	calculated parameters	
N	number of turns	48
R_{load}	load resistance	3.6 Ω
I_m	maximum phase current	166.6 A
A_C	core cross-section area	2000 mm^2
A_w	window cross-section area	7177.2 mm^2
l_N	length of the window area	451.11 mm
b	width of the window area	15.91 mm
l_g	airgap length	1 mm
w	width of the core	6.01 mm
R_{mean}	mean radius of winding	72.42 mm
l_c	conductor length	6.45 mm
R_1	outer radius of the first effective cross-section area A_{C1}	88.8 mm
ρ_C	resistivity of copper	1.72×10^{-8}Ωm
MLT	mean length of a turn	40.56 mm
	post-processing parameters	
P_1	copper loss	249.54 W
P_2	core loss	210.36 W
η	efficiency	98.8%
L_1	leakage inductance	17.37 µH
M	magnetizing inductance	6.237 mH

C. Simulation results and discussion

Fig. 3 shows the structure single-phase rotary transformer in 3D and 2D constructed in Ansys Maxwell. The transient solution type is used. Fig. 4 shows the external circuit that supplies the transformer and also connects it to the load during transient simulation. Assume an ideal condition, the primary series resistance is set as 0.01n Ω which can be neglected. The load resistance in the secondary is 3.6Ω.

In the 2D model, the model depth is set to 455 mm, which is the expansion of curve surface of 3D model. In other words, the 2D model depth is equal to the airgap perimeter of the 3D model.

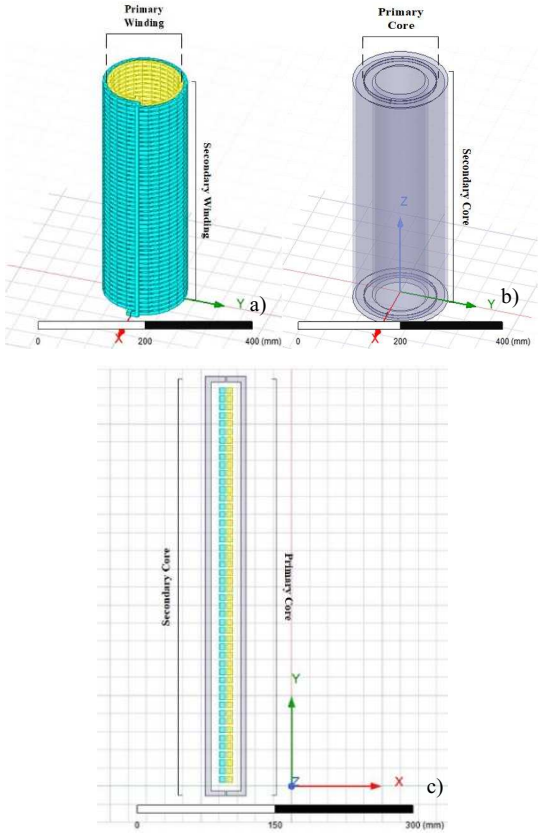

Fig. 3. Structure of single-phase rotary transformer. (a) Windings of 3D model (b) cores of 3D model (c) 2D model

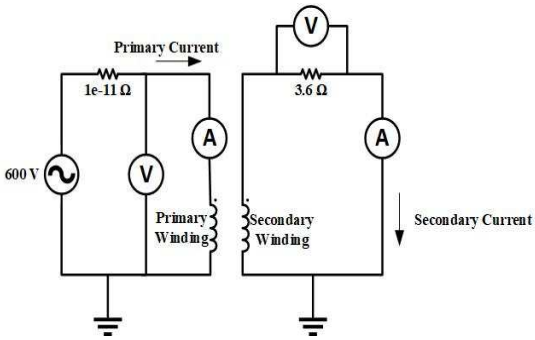

Fig. 4. External circuit used for simulations

Voltage and current results on the primary side and secondary side as well as the output power are presented in Fig. 5, Fig. 6 and Fig. 7.

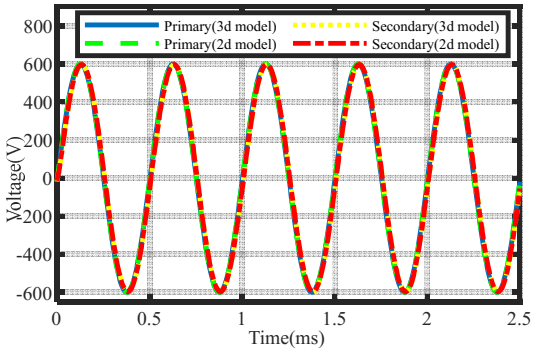

Fig. 5. Voltages of primary and secondary winding

From the simulation results of 2D and 3D, it is clear that 2D model simulation results are very close to 3D model.

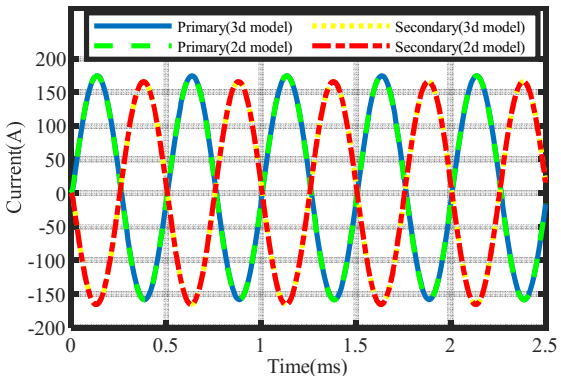

Fig. 6. Currents of primary and secondary windings

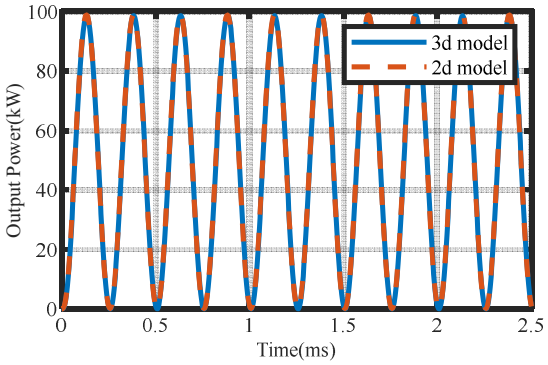

Fig. 7. Comparison of output power of 2D and 3D models

Fig. 8 shows the core loss as simulated by the FEM software, in both cases the instantaneous losses retain the same shape with the 3d model providing better understanding of the extra losses created by the curvature shape that is otherwise omitted in the 2d design. Considering these figures and comparing the results, it could be concluded that:

- The simulation results verify the analytical equations and the design procedure.
- 2D and 3D simulation results are very close so it is reasonable to use 2D model for sensitivity analysis as this reduced the required time and computational memory considerably.
- After 0.5ms, the circuit is in steady state, the maximum core loss of 3d model is nearly 50W more than that of 2d model, it is affected by the curve surface of 3d model.

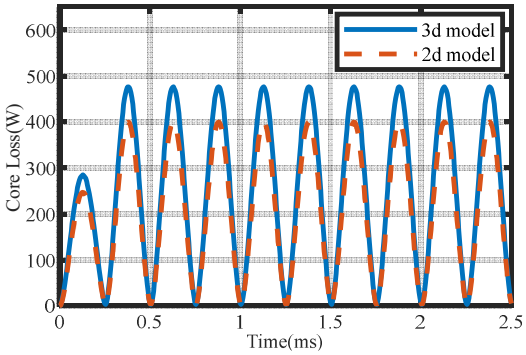

Fig. 8. Core loss comparison between 2D and 3D models

The magnetic flux density distribution at nominal power is shown for 2D and 3D model in Fig. 9, it shows the magnetic flux density does not exceed the operation flux density which implies that there is no saturation in the core.

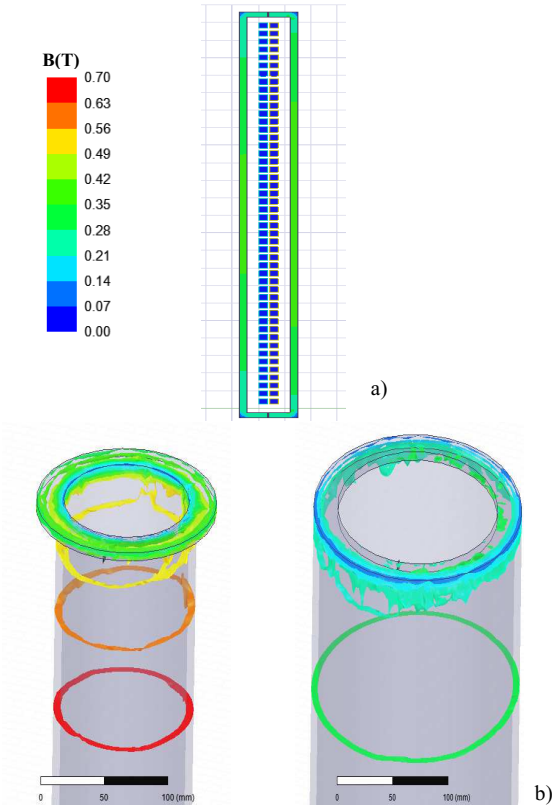

Fig. 9. Magnetic flux density: a) 2D model, b) 3D model

III. Sensitivity Analysis

A. Procedure

To evaluate the effect of some important parameters on the performance of the rotary transformer, sensitivity analysis was performed. The output power of the rotary transformer held constant at its rated value.

Between geometrical parameters, the airgap length and the winding window sizes are selected. Moreover, the operating flux density and current density are effective constants that considerably affect the performance and output characteristics of the rotary transformer.

B. Procedure

Fig. 10 shows the sensitivity analysis results for the losses and leakage inductances. As seen, the airgap length affects the copper loss and the leakage inductance directly but the core loss indirectly. This trends is similar for the working flux density as well as the winding window width. The effect of current density is different that means that it inversely affects the core loss, it is caused by the decrease of the conductor length.

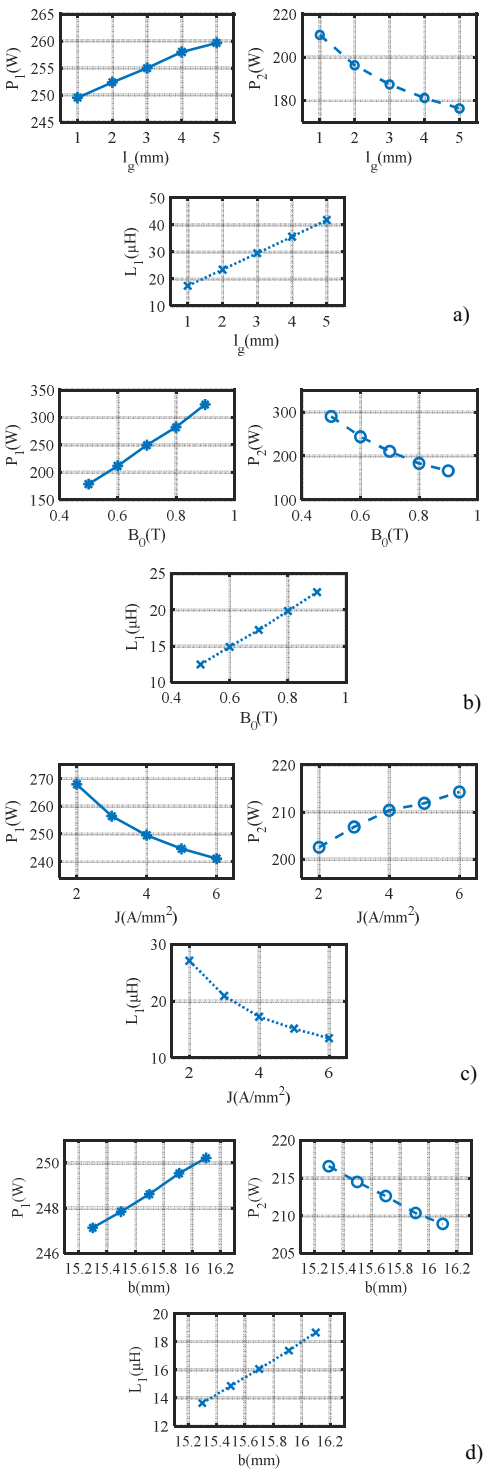

Fig. 10: sensitivity analysis: a) airgap, b) flux density, c) current density, d) winding window width

The analysis presented provides a vision to the design parameters and constraints of the rotary transformer based on the desired performance of the system. For example, to maximize the efficiency, these parameters should be selected or limited such that the losses become minimized.

Furthermore, it is evident that there is an order of magnitude difference in the copper loss calculation againt the losses obtained from the FEM simulation, this could be due to underestimation of numerical parameters. However the reported efficiency of the system is calculated based in the FEM simulations. Finally, this design procedure does not take into account the eddy and hysteresis losses which requiere more computational resources.

IV. Conclusions

In this paper the design and simulation of a high power single phase rotary transformer was done. As seen in the simulations, the power transfer efficiency is up to 98.8% which could be used as a replacement for the slip rings in high power applications like the X-rotor. The waveforms of voltage and current presented that were nearly the same for both 3D and 2D models. The maximum secondary side current was close to the numerical calculated value of 166.6 A, which validates the design procedure presented in the paper. For the magnetic field results, flux density at the core was smaller than the operating flux density density of 0.7 T, which means there is no staturation in the core. Then in a sensitivity analysis, the effect in performance of different parameters were studied. The next step in this research will be the optimization of the system considering input and output interfaces.

ACKNOWLEDGEMENT

This project has received funding from the EU H2020 under grant agreement No 101007135.

References

[1] C. Flannigan, J. Carroll, and W. Leithead, “Operations expenditure modelling of the X-rotor offshore wind turbine concept,” *Journal of Physics: Conference Series*, vol. 2265, no. 3, p. 032054, 2022.

[2] J. McMorland, C. Flannigan, J. Carroll, M. Collu, D. McMillan, W. Leithead, and A. Coraddu, “A review of operations and maintenance modelling with considerations for novel wind turbine concepts,” *Renewable and Sustainable Energy Reviews*, vol. 165, p. 112581, 2022.

[3] W. Leithead, A. Camciuc, A. K. Amiri, and J. Carroll, “The X-rotor offshore wind turbine concept,” *Journal of Physics: Conference Series*, vol. 1356, no. 1, p. 012031, 2019.

[4] Harry O. Ohmstedt, Senior Member IEEE, “Collector Ring Marking”, 1990.

[5] X. Zhu, B. Lin, L. Liu, and Y. Luan, “Power transfer performance and cutting force effects of contactless energy transfer system for rotary ultrasonic grinding,” *IEEE Transactions on Industrial Electronics*, vol. 63, no. 5, pp. 2785–2795, May 2016.

[6] C.-S. Wang, G. A. Covic, and O. H. Stielau, “Power transfer capability and bifurcation phenomena of loosely coupled inductive power transfer systems,” *IEEE Transactions on Industrial Electronics*, vol. 51, no. 1, pp. 148–157, Feb 2004.

[7] X. Zhu, B. Lin, and L. Liu, “Efficiency-based compensations and the mechanical load dependencies of rotary transformer for rotary ultrasonic machining applications,” *IET Power Electronics*, vol. 8, no. 6, pp. 986– 993, 2015.

[8] R. Manko, S. Čorović and D. Miljavec, "Analysis and Design of Rotary Transformer for Wireless Power Transmission," *2020 IEEE Problems of Automated Electrodrive. Theory and Practice (PAEP)*, 2020.

[9] S. Botha and N. Gule, “Design and evaluation of a laminated three-phase rotary transformer for DFIG applications,” *Energies*, vol. 15, no. 11, p. 4061, 2022.